Title

Online Thevenin Parameter Tracking Using Synchrophasor Data

Authors

Jamei, Mahdi
Scaglione, Anna
Roberts, Ciaran
et al.

Publication Date

2017-02-05

Peer reviewed

Online Thevenin Parameter Tracking Using Synchrophasor Data

Mahdi Jamei, Anna Scaglione, Ciaran Roberts, Alex McEachern,
Emma Stewart, Sean Peisert, Chuck McParland

***Abstract*—There is significant interest in smart grid analytics based on phasor measurement data. One application is estimation of the Thevenin equivalent model of the grid from local measurements. In this paper, we propose methods using phasor measurement data to track Thevenin parameters at substations delivering power to both an unbalanced and balanced feeder. We show that for an unbalanced grid, it is possible to estimate the Thevenin parameters at each instant of time using only instantaneous phasor measurements. For balanced grids, we propose a method that is well-suited for online applications when the data is highly temporally-correlated over a short window of time. The effectiveness of the two methods is tested via simulation for two use-cases, one for monitoring voltage stability and the other for identifying cyber attackers performing "reconnaissance" in a distribution substation.**

***Index Terms*—Thevenin Parameters, Phasor Measurement Unit (PMU), Anomaly Detection, Cybersecurity.**

I. Introduction

The notion of a *Thevenin equivalent model* is widely used in power system for applications such as short circuit studies, determining the source equivalent impedance of the transmission grid, capacitor bank design [1], and stability monitoring. The Thevenin equivalent model provides insights on circuit behavior at specific points of interest, without detailed modeling of the full grid.

Many studies focus on estimating Thevenin parameters from field sensors, such as Phasor Measurement Units (PMUs). Most of these studies are at the transmission level, where the grid is typically balanced. Vu et al. [2] used the linear, least-square method to solve for the Thevenin parameters and employed the Thevenin impedance to apparent load impedance ratio (well-known L-index) to monitor the voltage stability margin. Using two consecutive phasor measurements, Smon et al. [3] employ Tellegen's theorem and the notion of adjoint networks to estimate the Thevenin circuit and apply this analytic to monitor grid stability. Tsai et al. [4] use recursive least-square to estimate Thevenin parameters and track the voltage stability margin. Corsi et al. [5] propose adaptive identification of Thevenin voltage and impedance equivalents with real-time voltage instability monitoring purposes. Wang et al. [6] estimate the equivalent Thevenin circuit of generators and incorporate the estimated model to extend the traditional L-index. Yuan et al. [7] conduct a comparative study between different PMU-based methods of Thevenin equivalents identification in terms of how fast and accurate each method is. Others [8], [9] identify the adverse effect of quasi steady-state condition in the grid on Thevenin parameter estimation, and propose to estimate the off-nominal frequency and compensate for this phenomena to obtain accurate solutions. The authors in [1], [10] estimate the Thevenin parameters in a non-linear least-square setting considering the variations of the Thevenin voltage source angle. Using measurements from a load busbar in an unbalanced distribution grid, Hart [11] proposes a method that requires only RMS values of the voltage to estimate the Thevenin circuit in a three-phase, 3- or 4-wire system.

In this paper, using the synchrophasor voltage and current measurements at the substation, we propose methods for estimating the Thevenin source impedance and voltage corresponding to substations delivering power to an unbalanced and balanced feeder. The advent of "micro-PMU" (μPMU) sensors, which measure the three-phase voltage and current phasor at different points over the distribution grid [12], enables analytics that are similar to the ones at the transmission level. However, the extension to the distribution grid requires care, as distribution feeders are typically unbalanced. In the unbalanced case, we take advantage of having non-zero negative and zero sequence to estimate not only the voltage and positive sequence impedance but also the zero sequence source impedance. It should be noted that the use of synchrophasor data for Thevenin estimation is a side benefit of PMUs but it does not mean that obtaining required input data for Thevenin estimation is not possible with current facilities other than PMUs.

In the case of balanced grid, we propose a new method that is effective even when the system of equations are close to be rank-deficient. In our proposed approach, only the magnitude of the Thevenin voltage and Thevenin impedance are assumed to be constant over a short window, and no assumption is made about the angle of the Thevenin voltage source. This in fact improves the results as compared to the methods that require the Thevenin voltage angle to be constant over a window of samples; an assumption that is not valid in practice. In this sense, our work is similar to the proposed

This research was supported in part by the Director, Office of Electricity Delivery and Energy Reliability, Cybersecurity for Energy Delivery Systems program, of the U.S. Department of Energy, under contracts DE-AC02-05CH11231 and DEOE0000780. Any opinions, and findings expressed in this material are those of the authors and do not necessarily reflect those of the sponsors.). M. Jamei and A. Scaglione are with the School of Electrical, Computer and Energy Engineering, Arizona State University, Tempe, AZ, USA. Emails: {mjamei, ascaglio}@asu.edu. C. Roberts, E. Stewart, S. Peisert, and C. McParland are with the Lawrence Berkeley National Laboratory, Berkeley, CA, USA. Emails: {cmroberts, estewart, sppeisert, cpmcparland}@lbl.gov. A. McEachern is the CEO of the Power Standards Lab, Alameda, CA, USA. Email: Alex@McEachern.com.

methods in [1], [10]. We show how our method is successful in tracking the voltage stability index on a load point at the transmission level. In addition, given growing concerns about the security vulnerabilities of network-connected control systems in the distribution grid, we show, through an example, how our Thevenin estimation can be useful to detect specific types of cyber-attacks in a distribution substation. Specifically, in this paper, we discuss the detection of certain types of *reconnaissance* activity over SCADA network by attackers—that is, subtle probes and manipulation of network-connected substation components by an attacker to test degree of access and possible broader physical impact on the distribution grid.

II. Thevenin Equivalent Estimation

Fig. 1 shows the Thevenin equivalent circuit as seen from bus 1. This could be a subtransmission or distribution substation. Due to the integration of PMUs at the transmission level and μPMUs at the distribution level, measurements of the three-phase voltage phasor, $\mathbf{v}[k]$, and the three-phase current phasor, $\mathbf{i}[k]$, are now available at bus 1 at a very high rate. In

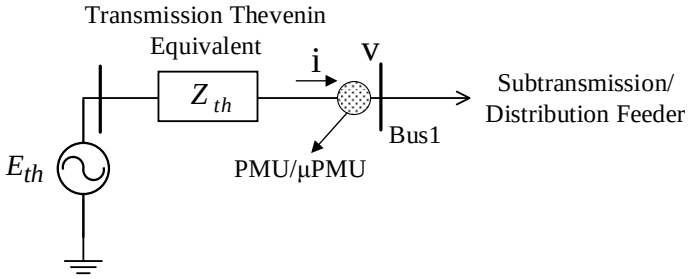

Fig. 1. Transmission Grid Thevenin Equivalent Seen from Substation

steady-state, the following equation holds for the circuit:

$$\mathbf{v}[k] = \mathbf{E}_{th}[k] - \mathbf{Z}_{th}[k]\mathbf{i}[k] \tag{1}$$

Equivalently, in the sequence domain, we have:

$$\mathbf{v}_s[k] = \mathbf{E}_s[k] - \mathbf{Z}_s[k]\mathbf{i}_s[k] \tag{2}$$

Assuming transposed lines implies that the mutual coupling between the zero, positive and negative sequence impedance at transmission level is zero. Hence, $\mathbf{Z}_s$ has the following form:

$$\mathbf{Z}_s = \begin{bmatrix} Z_0 & 0 & 0 \\ 0 & Z_1 & 0 \\ 0 & 0 & Z_2 \end{bmatrix} \tag{3}$$

In addition, since $\mathbf{E}_{th}$ is representing the generators voltage at the transmission, it can be considered to be balanced, and therefore can be written in the sequence domain as:

$$\mathbf{E}_s[k] = \begin{bmatrix} 0 \\ E_1[k] \\ 0 \end{bmatrix} \tag{4}$$

Therefore, we obtain the well-known decoupled set of equations as follows:

$$\begin{bmatrix} v_0[k] \\ v_1[k] \\ v_2[k] \end{bmatrix} = \begin{bmatrix} 0 \\ E_1[k] \\ 0 \end{bmatrix} - \begin{bmatrix} Z_0[k] & 0 & 0 \\ 0 & Z_1[k] & 0 \\ 0 & 0 & Z_2[k] \end{bmatrix} \begin{bmatrix} i_0[k] \\ i_1[k] \\ i_2[k] \end{bmatrix}. \tag{5}$$

A. Unbalanced Grid

Clearly, from (5), if the feeder connected to the substation is unbalanced (that is the case most of the times in the distribution feeders), all the Thevenin parameters can be estimated at each instant of time using the fact that $Z_1[k] \approx Z_2[k]$:

$$\begin{aligned} Z_0[k] &= -\frac{v_0[k]}{i_0[k]}, \quad Z_1[k] = -\frac{v_2[k]}{i_2[k]}, \\ E_1[k] &= \frac{v_1[k]i_2[k] - v_2[k]i_1[k]}{i_2[k]}. \end{aligned} \tag{6}$$

In this formulation we are taking full advantage of the inherent unbalanced behavior of the distribution grid that is usually considered a complication for many other applications. In this context, this feature allows us to update our estimation with the same frequency as the μPMU output rate. In addition, we are not only estimating the positive sequence impedance but also the zero sequence impedance. It should be noted that in some cases such as when the μPMU is placed after a Wye-Delta distribution transformer, the zero sequence current, i_0 is zero at point of measurement, which means that the zero sequence source impedance is infinite as expected.

B. Balanced Grid

When the grid is balanced, which is usually the case at the substations connecting the transmission grid to a subtransmission circuit, the method discussed above does not work. In this case, the only non-trivial equation in (5) is:

$$v_1[k] = E_1[k] - Z_1[k]i_1[k] \tag{7}$$

Clearly, what we have in (7) is a single equation with two unknowns, $E_1[k]$ and $Z_1[k]$, which does not have a unique solution. Therefore, we need to make appropriate approximations. Without loss of generality, we set the voltage phasor angle in (7) to zero and accordingly all the angles are reported relative to the voltage phasor angle. We drop the subscripts in (7) for simplicity of notation in the rest of this section. They will be reintroduced in the next sections.

Replacing the load in Fig. 1 with an equivalent apparent load impedance $Z_L = R_L + jX_L$ and neglecting the Thevenin resistance of the transmission grid in comparison with the Thevenin reactance, the corresponding phasor diagram is illustrated in Fig. 2. It is worth to mention here that the effect

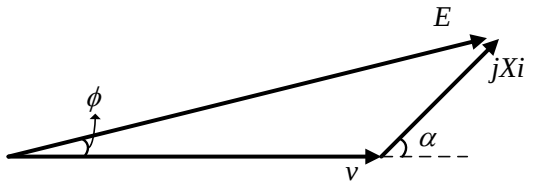

Fig. 2. Phasor Diagram of the Equivalent Thevenin Circuit in Fig. 1 for Balanced Grid.

of off-nominal frequency is an equal rotation in the vectors of the phasor diagram. Since we report the phasor angles relative to the voltage, this modulation term is accordingly removed from the voltage, current and the modeled Thevenin voltage source. We propose to use the following relationship based on

the phasor diagram in Fig. 2. Let $A[k] = |E[k]|$ and i_{im} be the imaginary component of the current, then we have:

$$\underbrace{A^2[k] - v^2[k] - X^2[k]|i[k]|^2 + 2i_{im}[k]X[k]v[k]}_{r(A,X;k)} = 0 \quad (8)$$

At each instant of time, there are infinite solutions for A and X as zeros of the "residual function" r. Assuming that A and X are constant over a window of M samples, and there is sufficient change in the feeder over this window, we form the following over-determined homogeneous set of equations:

$$\underbrace{\begin{pmatrix} r(A,X;k-M+1) \\ r(A,X;k-M+2) \\ \vdots \\ r(A,X;k) \end{pmatrix}}_{\vec{\mathbf{r}}(A,X;k)} = \begin{pmatrix} 0 \\ 0 \\ \vdots \\ 0 \end{pmatrix} \quad (9)$$

Note that we do not assume the angle ϕ is constant, and the assumptions made pertain exclusively to the Thevenin voltage magnitude and source reactance, which are considered constant over the examined window. Having constant voltage magnitude is reasonable since the Thevenin voltage source is representing the bulk grid, whose automatic voltage regulators operate on time-scales longer than those examined here. Our problem now translates into solving M non-linear quadratic equations. Taking the squared-norm of the residual vector, $\vec{\mathbf{r}}(A,X;k)$, in (9), we form the following objective function:

$$f(A,X;k) = \frac{1}{2}||\vec{\mathbf{r}}(A,X;k)||^2 \quad (10)$$

which is aimed to be minimized:

$$\min_{\boldsymbol{\theta}[k]} f(A,X;k) \quad (11)$$

where $\boldsymbol{\theta}[k] = [A[k], X[k]]^T$. The Levenberg-Marquardt Algorithm (LMA) is used to solve the non-linear least square problem. This method replaces the line search method in Gauss-Newton with a trust region strategy. The LMA overcomes one of the weaknesses of Gauss-Newton, i.e., the behavior when the Jacobian matrix of the residual vector is rank-deficient, or is close to be rank-deficient [13]. This is important in tracking the Thevenin parameter online since the change in the data during some intervals may return a Jacobian matrix which is ill-conditioned. The other advantage of the LMA as opposed to the Gauss-Newton is when the initial guess is far from the minimizer. In this case, Gauss-Newton converges very slowly or may not converge at all but LMA is proved to perform better under certain conditions. The implementation of the LMA in our system is shown in Algorithm. 1.

Note that in calculating $\mathbf{P}_{LM}$, we have used an ellipsoidal trust region in place of a spherical trust region by using the term $\lambda \text{diag}(\mathbf{J}^T\mathbf{J})$ instead of $\lambda\mathcal{I}$ as suggested in [14], where $\mathcal{I}$ is the identity matrix. The reason is that our problem is poorly scaled, or in other words the range of A and X are so different, and therefore we may face numerical difficulties or produce solutions with poor quality. The initial guess at time instant k can be provided by the estimated parameters at time instant k-1, i.e., $\boldsymbol{\theta}_0[k] \leftarrow \boldsymbol{\theta}[k-1]$.

Algorithm 1: Levenberg-Marquardt Algorithm (LMA) at time instant k

Input: $\vec{\mathbf{r}}(A,X;k)$, and an initial guess $\boldsymbol{\theta}_0[k]$
Output: Thevenin parameters at time k
begin
  flag=1;
  initialize $\rho < 1$, λ, and ϵ ;
  $\boldsymbol{\theta}[k] \leftarrow \boldsymbol{\theta}_0[k]$;
  while *flag==1* **do**
    $\mathbf{J} = \nabla\vec{\mathbf{r}}(\boldsymbol{\theta};k)$;
    $\mathbf{P}_{LM} = -(\mathbf{J}^T\mathbf{J} + \lambda\text{diag}(\mathbf{J}^T\mathbf{J}))^{-1}\mathbf{J}^T\vec{\mathbf{r}}(\boldsymbol{\theta};k)$;
    $\boldsymbol{\theta}_{new}[k] \leftarrow \boldsymbol{\theta}[k] + \mathbf{P}_{LM}$;
    if $f(\boldsymbol{\theta}_{new};k) < f(\boldsymbol{\theta};k)$ **then**
      $\lambda \leftarrow \rho\lambda$;
      $\boldsymbol{\theta}[k] \leftarrow \boldsymbol{\theta}_{new}[k]$;
    else
      $\lambda \leftarrow \frac{\lambda}{\rho}$;
    if $f(\boldsymbol{\theta};k) < \epsilon$ **then**
      flag $\leftarrow 0$;
  $\phi[k] = \sin^{-1}(X[k]i_r[k]/A[k])$
  return $E[k]$, $X[k]$;

Compared to the methods in [1], [10], our formulation leads to a smaller size of the Jacobian matrix, and therefore is computationally more efficient. Also, the mentioned advantages of LMA over the Gauss-Newton method used in [1] still remains.

III. Thevenin Estimation Results

In this section, we present the performance of the proposed Thevenin estimation through the numerical results for both cases of unbalanced and balanced grid.

A. Unbalanced Grid Thevenin Parameter Estimation

We modified IEEE-34 test case for our simulation by connecting it to a voltage source through a lumped transmission line representing the Thevenin impedance as shown in Fig. 3. The simulation is done in the DIgSILENT software [15] with phasor report rate of 120 Hz. We intentionally

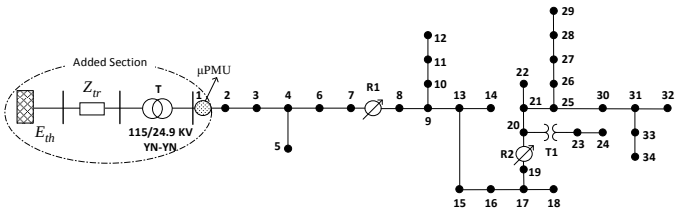

Fig. 3. Modified IEEE-34 Bus Test Case One-Line Diagram.

imposed the grid to work at off-nominal frequency of 59.9 Hz to simultaneously examine the effect of the off-nominal frequency on our estimation performance. We expect that our methodology for unbalanced grid will not be affected by off-nominal frequency because the estimation at each instant of time only uses the samples at that time. Table. I shows the estimated values for positive and zero sequence versus the actual ones. The estimated values are very close to the actual,

TABLE I
ACTUAL VS ESTIMATED THEVENIN SEQUENCE IMPEDANCE

	Estimated	Actual
Z_0	$2.5533 + j9.4392$	$2.5716 + j9.4320$
Z_1	$2.9922 + j10.92$	$2.99 + j10.8901$

which indicates the successful performance of the estimation. Fig. 4 shows the magnitude and the angle of the estimated Thevenin voltage versus the actual values captured from the simulation. As can be seen, the estimation of the Thevenin voltage is successful, and our algorithm tracks the parameters even when the off-nominal frequency is non-negligible, which is clear from the voltage angle.

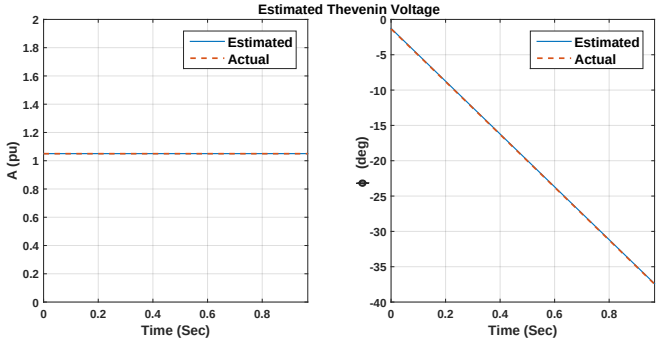

Fig. 4. Estimated Thevenin Voltage for Modified IEEE-34 Bus Under Off-Nominal Frequency.

B. Balanced Grid Thevenin Parameter Estimation

In balanced case, we first simulated the 39-Bus New-England dynamic model [16] using DIgSILENT software with a phasor report rate of 120 Hz. A very slow load ramping event of $+2\%$/sec is defined at load 16, while other loads are kept constant. The reason of the slow ramping event is to show how our method is suitable even under slow changes that is necessary for online application since large changes may not always happen over a short window. Taking a sliding window of 30 samples, i.e., $M = 30$, Fig. 5 shows the estimated versus actual value of the Thevenin impedance seen from bus 16. This window corresponds to 0.25 sec, where the assumption of constant Thevenin voltage magnitude is valid with a very good approximation. As can be seen, the estimates are very close

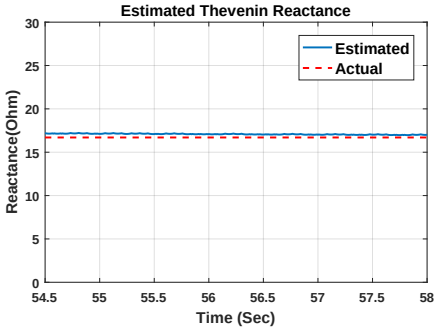

Fig. 5. Estimated Thevenin Reactance Seen from Bus 16 of New England Test Case Using LMA Method.

to the actual values, which indicate that the LMA method can successfully track the Thevenin parameters. We attribute the small residual error to the fact that we neglect the resistance.

Using the same sliding window size, the performance of the linear least-square method under this slow rate of change is illustrated in Fig. 6. As shown, this method completely fails to track the actual value of the Thevenin reactance in this scenario. The reason is most probably due to the fact that the phase angle is assumed to be constant over the window of samples.

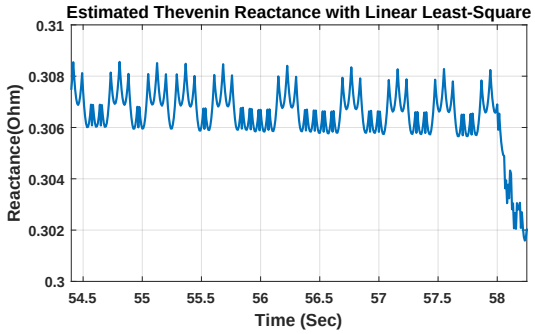

Fig. 6. Estimated Thevenin Reactance Seen from Bus 16 of New England Test Case Using Linear Least Square Method.

C. Voltage Stability Index Monitoring

An important application of the online Thevenin estimation algorithm is to monitor the voltage stability index at a load point in the transmission level. We use the voltage stability index in (12) that is employed in [2] to test the effectiveness of our Thevenin tracking method for a balanced grid. The index is defined as follows:

$$L[k] = \frac{X_1[k]}{|Z_L[k]|} = \frac{X_1[k]|i_1[k]|}{v_1[k]} \tag{12}$$

where $Z_L[k]$ is the apparent load impedance at time k. Based on (12), the stable and unstable regions are defined as follows:

$$\begin{cases} \text{Stable Region} & \text{if } L[k] \leq 1 \\ \text{Unstable Region} & \text{if } L[k] > 1 \end{cases} \tag{13}$$

For the numerical result, a ramping load event with load steps of $+18\%$/sec is introduced at all the load buses of the New-England 39 Bus test case until the grid goes unstable. Fig. 7(a)

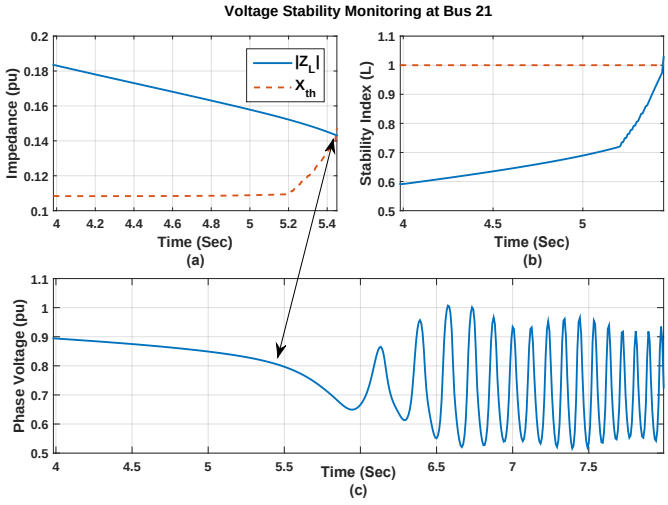

Fig. 7. Voltage Stability Index Monitoring at Bus 21.

shows the estimated Thevenin impedance and the magnitude of the apparent impedance. The voltage stability index (L) is also shown in Fig. 7(b). From the figure it is evident that the oscillation in the voltage starts when the magnitude of the apparent impedance meets the estimated Thevenin impedance or, equivalently, when the voltage stability index (L) crosses 1. This point corresponds to the maximum loadability of the system and the grid goes unstable beyond that. This is another indication that the Thevenin parameter is being tracked correctly, due to L correctly determining the point of maximum loadability.

D. Reconnaissance Attack Identification

In this use-case we assume that the substation connected to the distribution feeder is equipped with a normally-open spare transformer parallel to the main transformer, to restore the delivery of the power to the feeder when the main transformer fails or requires maintenance. Inserting the spare transformer into service, while the main transformer is also in service, has no adverse effect on the delivery of the power to the feeder downstream. It is therefore appealing for an attacker to try and test its ability to control the network through a compromised SCADA network, by changing the service status of the backup transformer switch when the main transformer is in service. The attacker may then mask this control action by spoofing the SCADA packages sent to the control center. The question is "can we detect such an activity with μPMU data?"

Suppose that we have a μPMU placed at the head of distribution feeder as shown in Fig. 8. In this circuit, the dominant term in the Thevenin source impedance would be due to the transformer impedance. Therefore, when the spare transformer switch is toggled maliciously, while the main transformer is in service, the source impedance will roughly reduces to half of its normal value. We propose to track the fast changes in the estimated positive sequence of the Thevenin source impedance. When a fast change is found, the magnitude of the change can be extracted to determine whether it can be attributed to the spare transformer switch or not. From

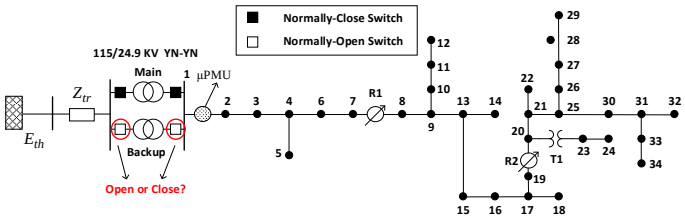

Fig. 8. Modified IEEE-34 Test Case for Reconnaissance Attack Identification

Fig. 9, when the switch gets closed the estimated impedance is almost half of what it was before. Considering the fact that the dominant term is due to the transformer and such a change cannot be the consequence of change in the transmission grid topology, the most plausible cause is the event that the spare transformer switch was closed. Once such a change has been detected, the control center is notified to determine if the change was a scheduled switch or an unexpected switch, potentially indicating malicious behavior.

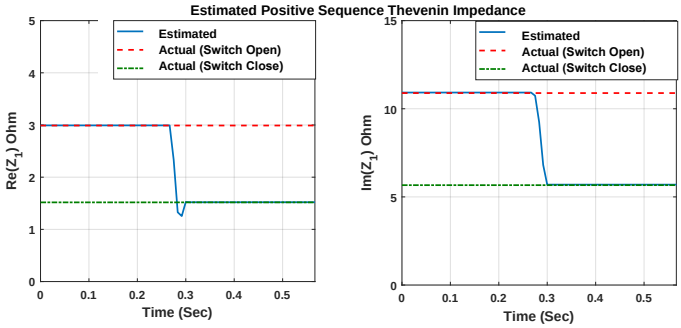

Fig. 9. Online Tracking of the Thevenin Source Impedance using μPMU Measurements

IV. Conclusion

In this paper, we have incorporated the synchrophasor data in the substation to estimate the source Thevenin parameters in real-time at the transmission and the distribution level. Our methodology for the balanced feeder is successful even when the data in the window of estimation has high temporal correlation and when there is a significant off-nominal frequency bias, as shown by our numerical analysis. These methods enable monitoring of the voltage stability margin and identification of certain types of "reconnaissance" by cyber-attackers.

References

[1] S. A. Arefifar and W. Xu, "Online tracking of power system impedance parameters and field experiences," *IEEE Transactions on Power Delivery*, vol. 24, no. 4, pp. 1781–1788, 2009.

[2] K. Vu, M. M. Begovic, D. Novosel, and M. M. Saha, "Use of local measurements to estimate voltage-stability margin," *IEEE Transactions on Power Systems*, vol. 14, no. 3, pp. 1029–1035, 1999.

[3] I. Smon, G. Verbic, and F. Gubina, "Local voltage-stability index using Tellegen's theorem," *IEEE Transactions on Power Systems*, vol. 21, no. 3, pp. 1267–1275, 2006.

[4] S.-J. S. Tsai and K.-H. Wong, "On-line estimation of Thevenin equivalent with varying system states," in *Proc. Power and Energy Society General Meeting-Conversion and Delivery of Electrical Energy in the 21st Century*. IEEE, 2008, pp. 1–7.

[5] S. Corsi and G. N. Taranto, "A real-time voltage instability identification algorithm based on local phasor measurements," *IEEE Transactions on Power Systems*, vol. 23, no. 3, pp. 1271–1279, 2008.

[6] Y. Wang, C. Wang, F. Lin, W. Li, L. Y. Wang, and J. Zhao, "Incorporating generator equivalent model into voltage stability analysis," *IEEE Transactions on Power Systems*, vol. 28, no. 4, pp. 4857–4866, 2013.

[7] H. Yuan and F. Li, "A comparative study of measurement-based thevenin equivalents identification methods," in *Proc. North American Power Symposium (NAPS)*. IEEE, 2014, pp. 1–6.

[8] S. M. Abdelkader and D. J. Morrow, "Online tracking of Thévenin equivalent parameters using PMU measurements," *IEEE Transactions on Power Systems*, vol. 27, no. 2, pp. 975–983, 2012.

[9] B. Alinejad and H. K. Karegar, "On-line Thevenin impedance estimation based on PMU data and phase drift correction," *To Appear in IEEE Transactions on Smart Grid*.

[10] M. Parniani, J. H. Chow, L. Vanfretti, B. Bhargava, and A. Salazar, "Voltage stability analysis of a multiple-infeed load center using phasor measurement data," in *Power Systems Conference and Exposition, 2006. PSCE'06. 2006 IEEE PES*. IEEE, 2006, pp. 1299–1305.

[11] P. Hart, "Characterising the power system at a load busbar by measurement," in *IEE Proceedings C-Generation, Transmission and Distribution*, vol. 133, no. 2. IET, 1986, pp. 87–94.

[12] A. von Meier, D. Culler, A. McEachern, and R. Arghandeh, "Micro-synchrophasors for distribution systems," in *Proc. IEEE PES Innovative Smart Grid Technologies Conference (ISGT)*, 2014, pp. 1–5.

[13] J. Nocedal and S. Wright, *Numerical optimization*. Springer Science & Business Media, 2006.

[14] G. Seber and C. Wild, *Nonlinear regression*. Wiley, New York, 1989.

[15] D. P. F. Manual and D. PowerFactory, "Version 14.0," *DIgSILENT GmbH, Gomaringen, Germany*, 2009.

[16] A. Pai, *Energy function analysis for power system stability*. Springer Science & Business Media, 2012.